Water Biology and Security xxx (xxxx) xxx

Contents lists available at ScienceDirect

Water Biology and Security

journal homepage: www.keaipublishing.com/en/journals/water-biology-and-security

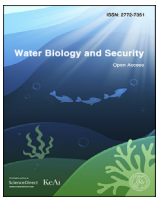

Research Article

Nuclear events during conjugation in the poorly studied model ciliate *Paramecium jenningsi*

Xue Zhang [a,1], Ruitao Gong [a,1], Yaohan Jiang [a,*], Xiaoteng Lu [b], Chenyin Wu [c], Lihan Wang [c], Hongwei Ma [c], Zhengxiang Zhang [c], Weibo Song [a,d], Khaled A.S. Al-Rasheid [e], Adriana Vallesi [f], Feng Gao [a,d]

[a] *Institute of Evolution & Marine Biodiversity, Ocean University of China, Qingdao, 266003, China*
[b] *Department of Biology, Shenzhen MSU-BIT University, Shenzhen, 518172, China*
[c] *College of Fisheries, Ocean University of China, Qingdao, 266003, China*
[d] *Laoshan Laboratory, Qingdao, 266237, China*
[e] *Zoology Department, College of Science, King Saud University, Riyadh, 11451, Saudi Arabia*
[f] *Laboratory of Eukaryotic Microbiology and Animal Biology, University of Camerino, Camerino, 62032, Italy*

ARTICLE INFO

Keywords:
Ciliates
Conjugation
Cytology
Life cycle
Nuclear events
Paramecium jenningsi

ABSTRACT

Ciliated protists are highly differentiated unicellular eukaryotes that possess special sexual processes (conjugation and autogamy) that rely on their unique nuclear dimorphism, i.e., the presence of both a germline micronucleus (MIC) and a somatic macronucleus (MAC) in a single cell. The sexual processes show a high diversity in different ciliates. To better understand the differentiation and evolution of sexual processes in closely related species, we investigated the nuclear events during conjugation in *Paramecium jenningsi* strain GZ, a poorly studied close relative of the well-known *P. aurelia* complex. The main results include: (1) the conjugation process takes about 48 h, including three prezygotic divisions (meiosis I, II, and mitosis) and three postzygotic divisions; (2) the MICs are dominated by the "parachute" phase at the prophase of meiosis I; (3) after meiosis II, a variable number of nuclei undergo the third prezygotic division, and the two products near the paroral cone become the genetically identical migratory and stationary pronuclei; (4) the synkaryon divides three times to form the MIC and the MAC anlagen, but only one nuclear product of the first postzygotic division completes the next two divisions; and (5) an extra cell division is required to complete the last step of conjugation, during which two MIC anlagen undergo mitotic division while two MAC anlagen are distributed between the daughter cells without division. The comparison of the nuclear events during conjugation in representatives of the class Oligohymenophorea reveals that usually there are three prezygotic divisions and a variable number of postzygotic divisions. However, the number of selected and differentiated nuclei after each division differs among species. This study provided a new model ciliate for further investigations of nuclear selection and differentiation as well as nuclear morphology during meiosis.

1. Introduction

The emergence of the sexual processes, which involve meiosis and fertilization, was the most critical step in the evolution of eukaryotes (Goodenough and Heitman, 2014; Bai, 2015). It is widely accepted that sex and sex differentiation were first established in unicellular eukaryotes (Cavalier-Smith, 2002; Chen et al., 2019; Knoll, 2014), and in this regard, ciliated protists represent good material to study the origin and evolution of sex.

Ciliated protists are the most specialized and differentiated unicellular eukaryotes, having high morphological and ecological diversity and wide distributions (Chi et al., 2022; Li et al., 2022; Lynn, 2008; Ma et al., 2022a, 2022b; Song et al., 2022; Wang et al., 2022). A distinct feature of ciliates is nuclear dimorphism, which means each cell possesses at least one micronucleus (MIC) and at least one macronucleus (MAC), although the number of nuclei can vary among species and life cycle stages (Duan

* Corresponding author.
E-mail address: jiangyaohan1993@163.com (Y. Jiang).
[1] These authors contributed equally to this work.

https://doi.org/10.1016/j.watbs.2023.100201
Received 10 March 2023; Received in revised form 17 June 2023; Accepted 3 July 2023
Available online xxxx

Please cite this article as: Zhang, X. et al., Nuclear events during conjugation in the poorly studied model ciliate *Paramecium jenningsi*, Water Biology and Security, https://doi.org/10.1016/j.watbs.2023.100201

et al., 2021; Fu et al., 2022; Sheng et al., 2020, 2021; Zhao et al., 2021; Zheng et al., 2020).

The DNA-rich MAC is transcriptionally active and expresses all the mRNAs required for vegetative growth, while the diploid MIC is transcriptionally silent but has a function in the construction of a normal-length cytopharynx during vegetative growth and is mainly active during sexual reproduction (Chau and Ng, 1988; Fujishima and Watanabe, 1981; Ng and Fujishima, 1989; Prescott, 1994).

Ciliates have a unique method of sexual reproduction known as conjugation (Phadke and Zufall, 2009). This process requires two partners of complementary mating types to cease vegetative growth and temporarily unite in mating pairs. During this period, the partners exchange gametic nuclei (Orias, 1986; Cervantes et al., 2013; Luporini et al., 2005, 2016). Conjugation in ciliates displays considerable variation among different species. The main variations include: (1) differences in the number and characteristics of MIC and MAC; (2) the sequence of mitosis and meiosis of the MIC, which determines whether the gamete nuclei are genetically identical or different; (3) the number of pre- and post-zygotic divisions, as well as the occurrence of nuclear degradation; (4) the occurrence of additional cell divisions required to complete the conjugation process; (5) the presence or absence of cell and nuclear fusion. Despite these variations in nuclear events, some aspects of the ciliate life cycle remain relatively conserved. For instance, both MIC and MAC develop from the zygotic nucleus, and the development of MAC involves a series of steps, including DNA elimination, chromosome fragmentation, and amplification (Gong et al., 2020, 2022; Jahn and Klobutcher, 2002; Jiang et al., 2019; Lipps et al., 2010; Prescott, 1994; Raikov, 1972; Zhang et al., 2022).

In *Paramecium*, a well-known model genus, conjugation processes and the mechanisms of mating type determination have been studied for about a century (Hiwatashi and Mikami, 1989; Orias et al., 2017). However, studies of sexual processes have focused on only a few species. In the present study, we investigated conjugation in *P. jenningsi* strain GZ, a species belonging to the "aurelia" subgroup together with the *P. aurelia* complex, which includes morphologically identical but reproductively isolated species (Aufderheide et al., 1983; Potekhin and Mayén-Estrada, 2020; Przyboś et al., 2015; Przyboś and Tarcz, 2016; Sonneborn, 1975). Although *P. jenningsi* (Fig. 1) is related quite closely to species of the *P. aurelia* complex based on molecular markers (Allen et al., 1983; Barth et al., 2008; Fokin et al., 2004; Yamauchi et al., 1995), phylogenetic relationships (Aury et al., 2006; Sawka-Gądek et al., 2021) and morphological characteristic (Sonneborn, 1975), it differs from these species in the sexual process (Fokin et al., 2001; Mitchell, 1962; Sonneborn, 1975).

Here, we provide a detailed photomicrographic description of the nuclear events and temporal sequences that take place during conjugation in *P. jenningsi* strain GZ, thereby filling the gaps in knowledge left by previous studies that comprise only textual descriptions (Fokin et al., 2001; Mitchell, 1962). In addition, we compared conjugation in *P. jenningsi* strain GZ with 23 other oligohymenophorean species encompassing symbiotic, facultative parasitic, sessile, and free-living lineages. The results of this study not only provide a new model system for investigating the molecular mechanism of gametic nuclei selection, but also increase our knowledge of nuclear differentiation, evolutionary relationships, and conservation and variability of meiosis in eukaryotes.

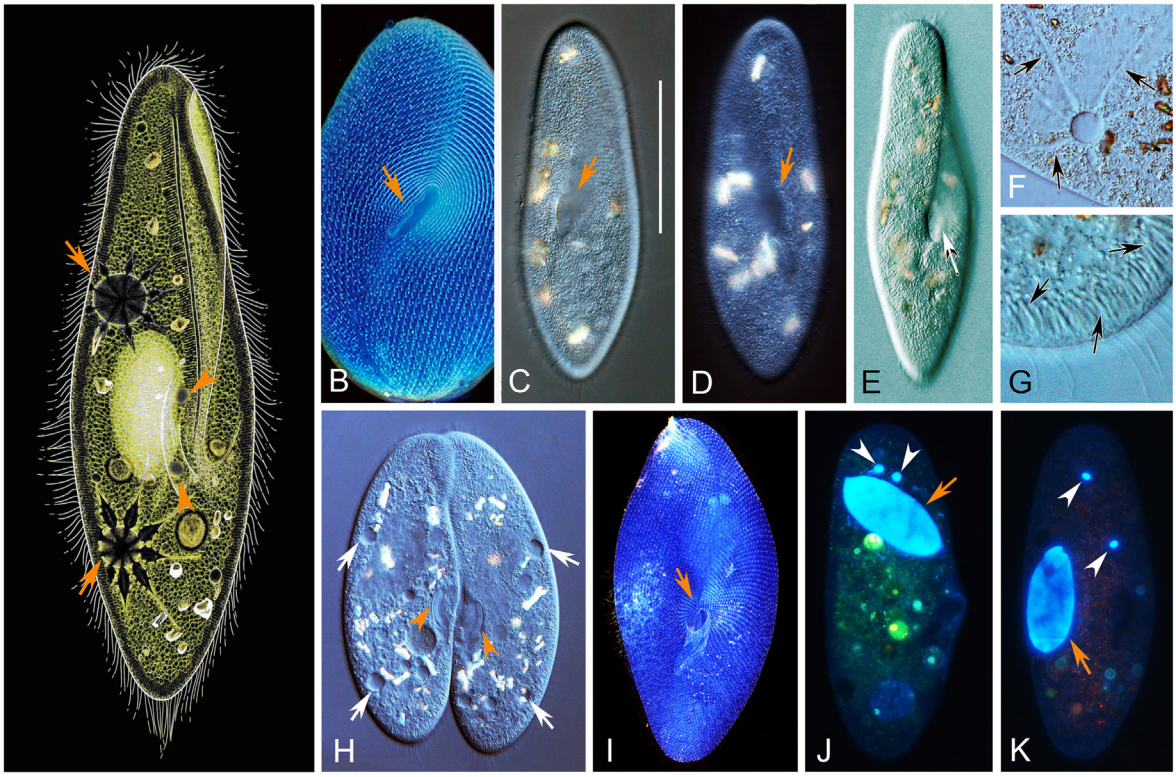

Fig. 1. Morphology of *Paramecium jenningsi* strain GZ. (**A**) Schematic diagram (modified from Zhang et al., 2022). Arrows indicate contractile vacuoles and arrowheads label micronuclei. (**B, I**) Ventral views to show the ciliary pattern and buccal area (arrow) after silver carbonate staining. Images have been processed by the invert function via Photoshop. (**C–E**) Ventral views in vivo, arrows indicate buccal field; (**F**) Details of a contractile vacuole and collecting canals (arrows). (**G**) Details of the cortex, arrows point to the extrusomes. (**H**) Morphology of a mating pair, arrows mark the contractile vacuoles, and arrowheads indicate the buccal areas. (**J, K**) The macronucleus (arrows) and micronuclei (arrowheads) of a vegetative individual (J) or an individual undergoing early micronuclear migration (K) are shown after fluorescence staining with Hoechst 33342 and acridine orange. Ma, macronucleus. Scale bar = 80 μm.

2. Materials and methods

2.1. Sample collection, identification, and mating type determination

The strain used in this work was isolated from freshwater collected from the Liede River (the pre-navigational channel of Pearl River), Guangzhou, China (N23°06'44", E113°19'49"), and was assigned to the species *Paramecium jenningsi* based on live observation, silver carbonate staining (Fig. 1A–I), and small subunit ribosomal RNA (SSU rRNA) gene sequencing (Diller and Earl, 1958). DNA extraction, PCR amplification, and SSU rRNA gene sequencing were performed according to Chi et al. (2022). The SSU rRNA gene sequence was submitted to GenBank with the accession number ON366386. Further analysis based on 16 DNA markers (both nuclear and mitochondrial), which as carried out according to Przyboś and Tarcz (2016), indicated that it is *P. trijenningsi,* which is a member of the *P. jenningsi* complex. The monoclonal strains (the offspring of a mating pair of *P. jenningsi* strain GZ), named PJD1, PJD2, PJD3, and PJD4, were isolated and used in the experiments. Two complementary mating types were identified by pairwise mixture of the monoclonal strains. The strains PJD1 and PJD2 belong to the same mating type, which are complementary to the mating type of strains PJD3 and PJD4. The cells were kept at 8 °C in a low-nutrient medium for about one year before this study, and only a few cells of each strain were picked to carrry out each experiment.

2.2. Cell culture and conjugation induction

Cells were precultured before inducing conjugation in 5% fresh lettuce juice diluted with the modified Dryl solution (Dryl, 1959), using KH_2PO_4 instead of NaH_2PO_4 (KDS). The medium was inoculated with *Klebsiella pneumoniae* one day before being used (Hiwatashi, 1968). After clarification of the culture medium, cells were in a state of mild starvation and undergo conjugative activity within 48 h. Conjugation was induced by mixing highly reactive cells of complementary mating types (Hiwatashi, 1968). The preculture and the whole conjugation process were carried out at 25 °C.

2.3. Conjugation and cell staining

The mixing time was considered as time 0. Mating pairs or postzygotic cells were collected every 15 min near the synkaryon formation stages, every hour during anlagen development, and every 30 min during other stages. Cells were stained with Hoechst 33342 (HO) (Beyotime Institute of Biotechnology, Jiangsu, China) and acridine orange (AO) (Shanghai Chemical Reagent Co., Ltd., Shanghai, China) (Yang et al., 2007). For every 100 μL cell suspensions, 1.8 μL of HO (stock solution: 2 mg/mL) or 0.8 μL of AO (stock solution: 100 μg/mL) were added. The mixtures were incubated at room temperature (ca. 25 °C) for 20 min and observed as previously described (Gong et al., 2020; Jiang et al., 2019; Zhang et al., 2022). For each nuclear stage, the state of nuclear events of 25 mating pairs or exconjugants were recorded to identify the dominant stage.

2.4. Phylogenetic analyses

A concatenated tree of the class Oligohymenophorea was constructed using the maximum likelihood (ML) method based on the SSU rRNA gene sequences, then the clades between subclass were adjusted according to the phylogenomic relationships analyzed in Wang et al. (2021). The SSU rRNA gene sequence of *P. jenningsi* (Acc. No. ON366386) was included in the phylogenetic analyses along with 24 other sequences obtained from the GenBank database. Two sequences of *Coleps* were selected as the outgroup. In order to determine the specific attribution of *P. jenningsi* strain GZ within the *P. jenningsi* complex, 11 nuclear DNA fragments and five mitochondrial DNA fragments of *P. jenningsi* strain GZ were extracted from the assembled (unpublished) genomic data by the BLAST algorithm with known *Paramecium* genes as selected by Przyboś and Tarcz (2016).

Sequences were aligned using the GUIDANCE2 Server (http://guidance.tau.ac.il/) with default parameters (Sela et al., 2015). The alignment was manually modified using BioEdit v.7.0.1 (Hall, 1999). Aligned sequences were concatenated using PhyloSuite (Zhang et al., 2020). ML analyses were performed in CIPRES Science Gateway (http://www.phylo.org/sub_sections/portal) (Miller et al., 2010). The ML tree was constructed using RAxML-HPC2 on XSEDE v.8.2.12 with the GTRGAMMA model and 1000 bootstrap replicates. Tree topologies were visualized with MEGA v.7.0.26 (Kumar et al., 2016).

3. Results

3.1. Formation of conjugant pairs and meiosis of the MIC (the first two prezygotic divisions)

Mild starvation induced sexual reactivity, preparing cells for conjugation. Autogamy was observed if the monoclonal cell lines were not mixed with the cells with complementary mating type. Selfing was not observed in either strain. After mixing different mating types, most cells clustered immediately, and large clumps of agglutinated cells formed within 20 min. Approximately 2 h after mixing, conjugant cells were firmly united in pairs that separated from the clumps (Fig. 2A).

In the stage preceding the formation of holdfast union, a significant repositioning of the two micronuclei was observed, termed early micronuclear migration (EMM) (Fujishima and Hiwatashi, 1977). The two micronuclei shifted from being adjacent to each other and being in close proximity to the macronucleus (Fig. 1J) to a noticeable displacement away both from each other and from the macronucleus (Figs. 1K and 2A). One hour after mixing, EMM occurred in approximately 95% of the cells. It is noteworthy that EMM had already occurred in cells with conjugation activity, even though they had not been mixed with cells of a complementary mating type (Fig. 1K). This observation may be associated with the capability of *P. jenningsi* for autogamy and provides further evidence that EMM serves as the initiating signal for fertilization (Fujishima and Hiwatashi, 1977).

With the onset of meiosis and during the first meiotic division (meiosis I), the two MICs of each cell partner enlarge, indicating that the MICs have entered the pre-meiotic "S" phase (Fig. 2B) (Fujishima, 1983). They then undergo complex morphological changes. Chromatin of the MICs gradually condenses and moves to one pole of each nucleus (Fig. 2C). As a result, the MICs look like drooping parachutes, formed by two different parts connected by filamentous chromatin fibers (Fig. 2D and E). This "parachute" shape of the nucleus is a typical marker of the zygotene stage (Raikov, 1982). The chromatin continues to condense and moves to the metaphase plate of meiosis I (Fig. 2F). Then, the two MICs complete meiosis I and produce four haploid nuclei (Fig. 2G, arrowheads). All four nuclear products immediately undergo meiosis II, resulting in eight daughter nuclei (Fig. 2H, arrowheads). While the first meiotic division lasts about 12 h, the second division takes about 1 h. The prezygotic divisions are thus completed in about 13 h after cell mixing (Fig. 4, Table S1), but they may be asynchronized in cells of the same conjugant pair.

3.2. Mitosis (the third prezygotic division) and synkaryon formation

After meiosis, cells undergo the third prezygotic division (mitosis). The number of haploid nuclei concluding the third prezygotic division is variable (1–5 in the present work) (Fig. 2I and J). However, the migratory and stationary pronuclei are always generated by the division of the nucleus in the proximity of the paroral cone. After mitosis, the stationary pronucleus remains near the paroral cone and the migratory pronucleus moves far away, while the other nuclei degenerate (Fig. 2I and J). The processes of mitosis and pronuclei formation take about 1.5 h (Fig. 4, Table S1). Next, the migratory pronuclei are exchanged between the two partner cells and fuse with the retained stationary pronuclei to form the

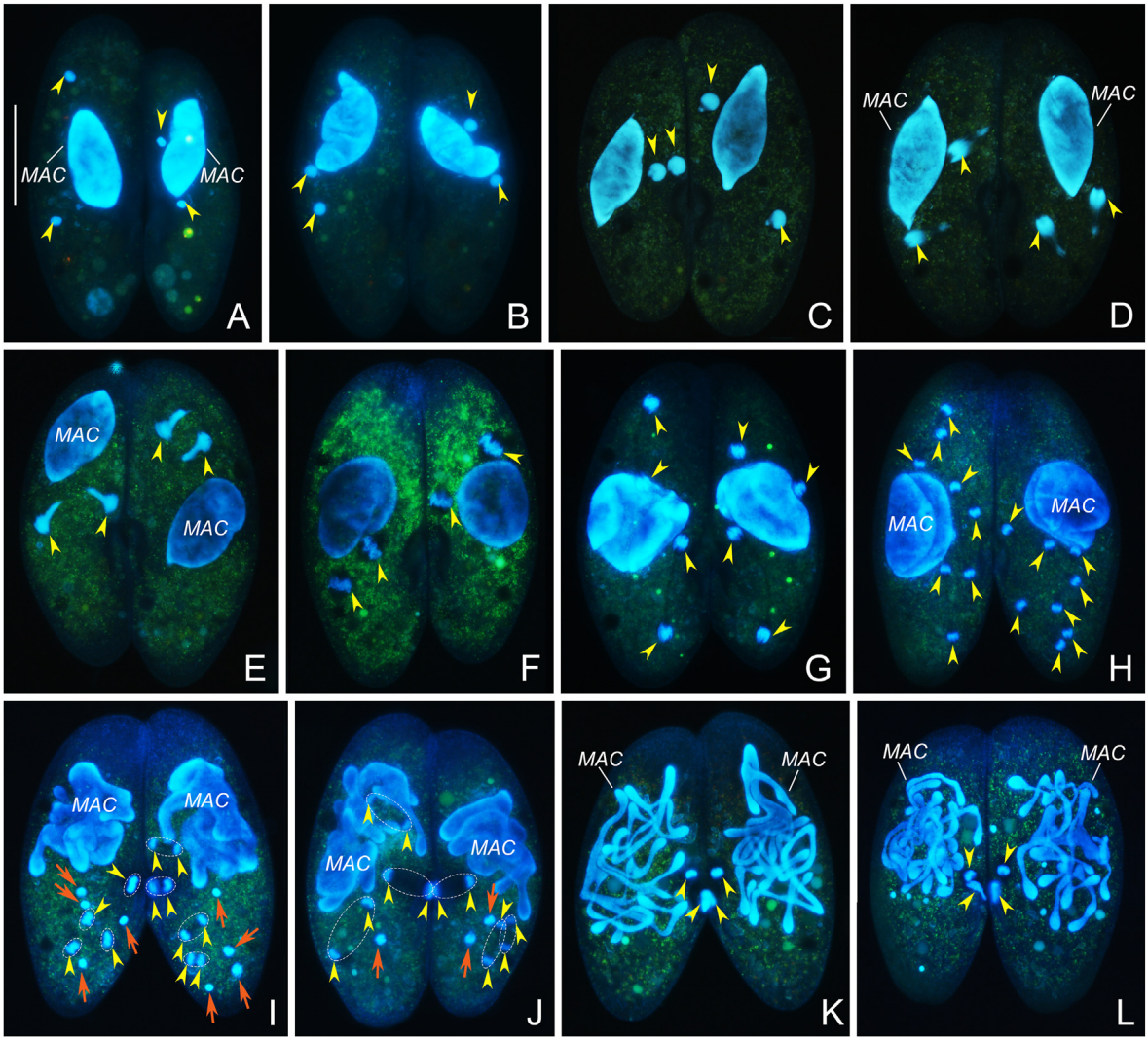

Fig. 2. Conjugating cells of *Paramecium jenningsi* strain GZ to show the nuclear events before synkaryon formation. Arrowheads (yellow): MIC or products of prezygotic divisions. Arrows (orange): degrading nucleus after the third prezygotic division. (**A**) Mating pair that has just formed and early micronuclear migration has occurred. (**B**) The MICs are enlarged. (**C**) The initial form of the "parachute" stage. (**D**) Typical "parachute" stage of MICs during the prophase of the first prezygotic division (meiosis I). (**E**) The chromatins move to the center of the nucleus and no longer maintain the typical "parachute" shape. (**F**) In the metaphase of the meiosis I, the chromosomes are neatly arranged. (**G**) The first prezygotic division is completed and four nuclear products are formed in each conjugant. (**H**) The second prezygotic division is completed and generates eight nuclear products. (**I**, **J**) Different numbers of nuclei, four in I and three in J, undergo the third prezygotic division (dashed ellipses). (**K**) Exchange of migratory pronuclei. (**L**) The migratory pronuclei have been exchanged but not fused with the stationary pronuclei of the counterpart cell. Scale bar = 60 μm.

synkaryons (Fig. 2K, L; Fig. 3A), which takes about 15 min (Fig. 4, Table S1).

3.3. Postzygotic divisions and development of new MIC and MAC anlagen

The synkaryon requires about 2.25 h to undergo three postzygotic divisions, which are successive mitotic divisions (Fig. 3A–F; Fig. 4). After the first postzygotic division, only one nuclear product completes the remaining two divisions and produces four nuclear products, while the other one degenerates (Fig. 3B and C). Mating pairs separate after the second postzygotic division (Fig. 3D).

Of the four nuclear products generated by the third postzygotic division, two develop into the new MICs, and the other two develop into the new MAC anlagen, which show more homogeneous staining than the parental MAC (Fig. 3G and H, arrows). It was observed that if food is not sufficient to support the following stages, the development of the MAC anlagen will stop and the morphology of the macronuclear anlagen would remain as shown in Fig. 3H. Eventually the cells will die.

The development of MAC anlagen and cell maturation require an additional cell division. The two MICs undergo mitosis and separate in the two daughter cells, while the two MAC anlagen are distributed between the daughter cells without division. Finally, each daughter cell has one MAC and two MICs, plus a few fragments of the parental MAC (Fig. 3I). These cells then enter the asexual phase of the lifecycle. The entire conjugation process takes about 48 h when the postzygotic cells were fed 33 h after mixing (Fig. 4, Table S1).

3.4. The destiny of the parental macronucleus

Morphological changes in the parental MAC from ellipsoidal to flat are visible as early as the metaphase of meiosis I (Fig. 2F). During the third prezygotic division, the MAC elongates gradually disintegrates into

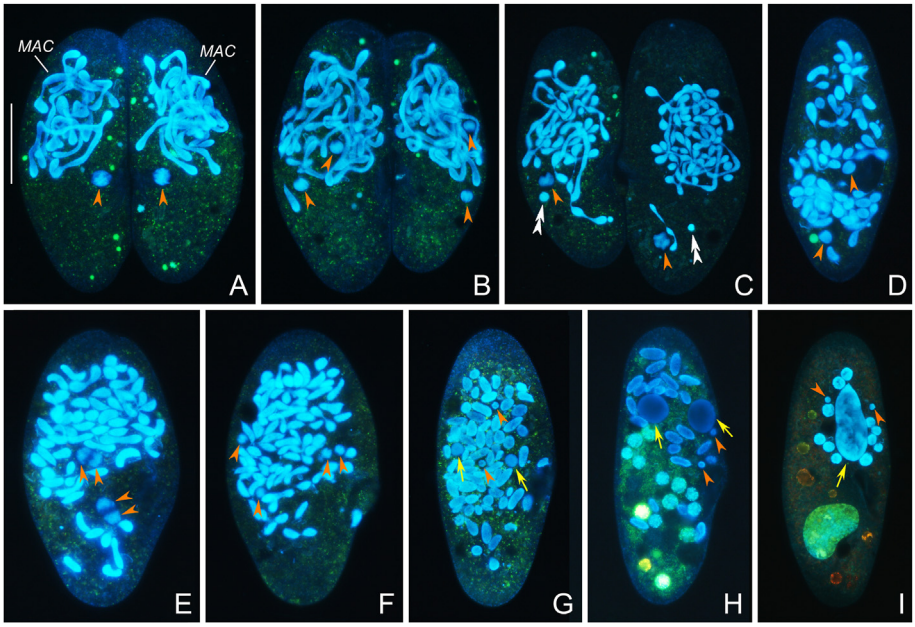

Fig. 3. Nuclear events after synkaryon formation in *Paramecium jenningsi* strain GZ. Arrowheads (orange): synkaryon, postzygotic division products, or new MIC. Arrows (yellow): new MAC anlagen. Double-arrowheads (white): degenerating synkaryon products. (**A**) The synkaryon stage. (**B**) The first postzygotic division. (**C**) One of the first postzygotic division products undergoes the second division while another is degenerating. (**D**) Separation of a mating pair and the second postzygotic division. (**E**) The third postzygotic division. (**F**) After the third postzygotic division, four nuclear products are retained in each cell. (**G, H**) Nuclear products of the third postzygotic division differentiate into MAC and MIC. (**I**) After cell division, two MICs, and one MAC remain in the cell, as well as degenerated fragments of the parental MAC. Scale bar = 60 μm.

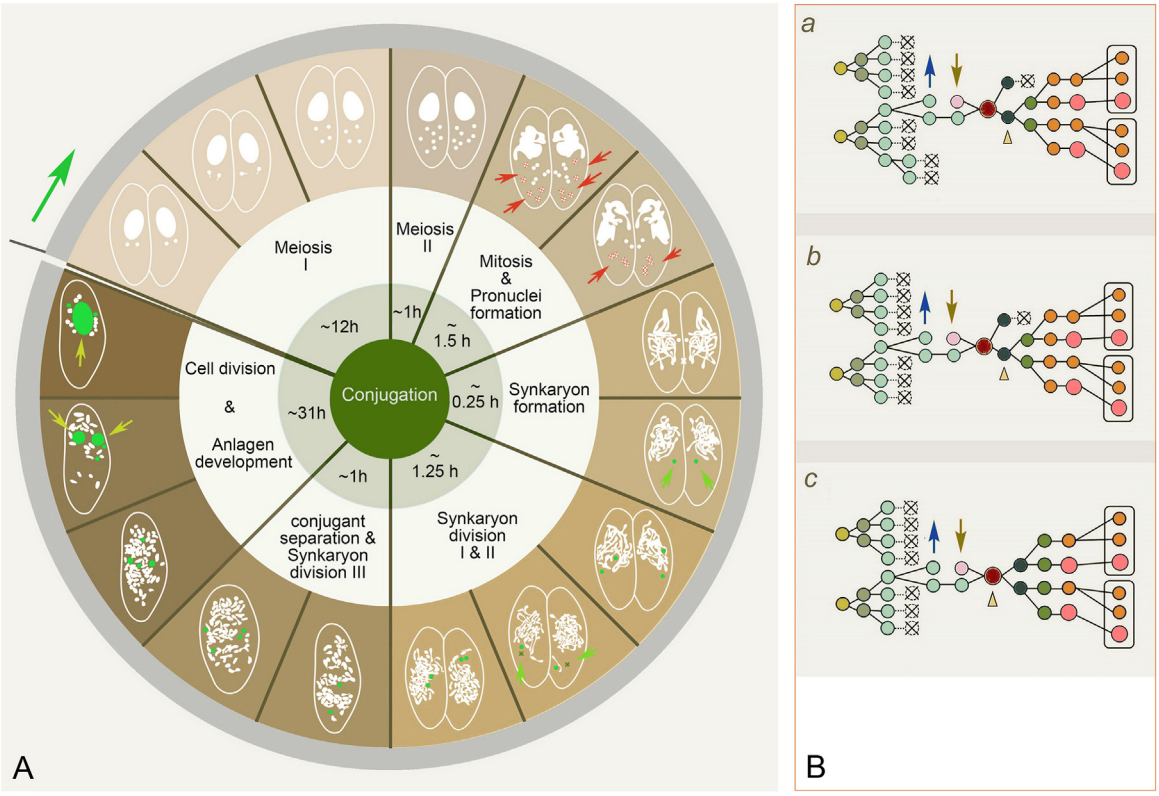

Fig. 4. Time-course analysis of nuclear events during conjugation in *Paramecium jenningsi* strain GZ. (**A**) Timing of nuclear events during conjugation. (**B**) Comparison of the nuclear events during conjugation in *P. jenningsi* (a, the present work and Mitchell, 1962, 1963; b, Fokin et al., 2001) and other sibling species in *P. aurelia* complex (c, Diller, 1936; Fokin et al., 2001; Sonneborn, 1938).

strips (Fig. 2I and J) which become entangled as the process of degradation continues (Fig. 2K, L; Fig. 3A–D). In exconjugants, the parental MAC becomes a multitude of dot-like and short rod fragments (Fig. 3D–G). These fragments continue to undergo programmed degradation and are finally depleted during the transition from the sexual to the asexual stage of the life cycle (Fig. 3H and I; Fig. 4).

4. Discussion

4.1. Nuclear selection and differentiation in paramecium during conjugation

In this study, we provide detailed documentation of the conjugation

process of *P. jenningsi* strain GZ through high-quality photomicrographs. Our findings shed light on the nuclear processes that occur during pre- and postzygotic nuclear divisions, providing a clearer understanding of the mechanisms involved. Notably, our observations reveal that before cell division, six rounds of nuclear divisions occur, but only certain nuclear products advance to subsequent stages, suggesting that programmed nuclear degradation and intracellular localization play key roles in nuclear selection.

4.1.1. Selection of haploid MICs (hMICs)

Although a variable number of hMICs undergos the third prezygotic division in *P. jenningsi* strain GZ (Fig. 2I and J), only the product located near the paroral cone forms the migratory and stationary pronuclei. This implies that the division of hMICs and pronuclei formation are independent events. Related studies in *Paramecium caudatum* have shown that hMICs are destined to degenerate, but the special environment of the paroral cone can recruit DNA repair proteins to rescue degeneration (Yanagi, 1987). In *Tetrahymena thermophila*, γH2AX, a protein marker for DNA double-strand breaks, has been shown to localize in the four products of prezygotic meiosis II, and to disappear in the finally selected hMIC, characterized by the presence of the marker for DNA repair H3K56ac (Chowdhury et al., 2005; Shi and Oberdoerffer, 2012). Recently, a more in-depth study of this process in *T. thermophila* showed that attachment of hMICs to the fused plasma membranes of conjugating cells is not a prerequisite for selection, but rather is a follow-up to the selection process (Akematsu et al., 2020). However, the location of selected hMICs is not completely random, as they tend to be more inclined to distribute between the MAC and the fused plasma membranes than unselected hMICs (Akematsu et al., 2020). Given that multiple hMICs were able to initiate and perform pre-gametogenic division, it was concluded that *P. jenningsi* strain GZ can, like *T. thermophila,* serve as a model system for studying the selection and differentiation of hMICs.

4.1.2. Nuclear dimorphic differentiation in exconjugants

As in *P. nephridiatum* (Jankowski, 1961), *P. calkinsi* (Nakata, 1956), and *P. bursaria* (Wichterman, 1948), one product of the first postzygotic division in *P. jenningsi* strain GZ degenerates while the remaining one undergoes and completes the subsequent postzygotic divisions to differentiate MICs and MACs in exconjugant cells. Indeed, the degeneration of pre-and/or postzygotic division products is a common occurrence in multiple *Paramecium* species and occurs at various specific stages. For example, in *P. bursaria*, degeneration takes place during the prezygotic division, while in *P. caudatum*, it occurs during the third postzygotic division prior to the differentiation of MIC and MAC anlagen (Wichterman, 1948; Yang et al., 2007). Insufficient attention has been given to the degeneration of the nucleus in the mentioned stages, leading to a lack of clarity regarding the factors that determine the distinct fates of the two products originating from the same division.

In comparison, the molecular mechanisms of nuclear differentiation have attracted more attention. Nuclear differentiation is an enigmatic process that involves nuclear fate decision and a high degree of genomic rearrangement (Akematsu et al., 2020; Kovalchuk, 2021; Orias, 1986). However, the mechanism by which the strikingly different fate of nuclei is determined during the differentiation of MIC and MAC anlagen has not been fully elucidated. The widely accepted hypothesis of nuclear differentiation states that the fate of nuclei depends on their localization in the cytoplasm, that is, cytoplasmic factors control nuclear activity (Mikami, 1980; Sonneborn, 1951). Studies on *P. caudatum* have shown that the differentiation of MAC anlagen or new MIC after the last postzygotic division depends on their transient relative position in the cytoplasm since the anterior nucleus becomes the MIC while all the posterior nuclei differentiate into MAC anlagen (Yanagi, 1987; Yang and Takahashi, 2000). In addition, the parental MAC may control the differentiation of the new MAC anlagen, underscoring the importance of nucleo-cytoplasmic interaction (Grandchamp and Beisson, 1981; Nanney, 1953a; Yang and Takahashi, 1999, 2002). In contrast to *P. caudatum*, the two postzygotic nuclei in the anterior region of the cell in *T. thermophila* develop into new MACs while the two in the posterior region differentiate into new MICs (Iwamoto et al., 2015; Nanney, 1953b). However, in *P. jenningsi* strain GZ, no distinct nuclear localization capable of influencing the fate of nuclei was observed (Fig. 3F–H). There was no particular lateral, vertical, or other specific orientation in which the nuclei were distributed either during and after the third postzygotic division or during the early stage of MAC and MIC anlagen differentiation (Fig. 3E–G). The difference of this feature among *P. jenningsi* strain GZ, *P. caudatum* and *T. thermophila* implies that *P. jenningsi* strain GZ could be a suitable model for investigating new mechanisms of MAC and MIC anlagen differentiation. How different signals, timing, spatial locations, and cellular contexts affect specific cell fate decisions will be the focus of future research.

4.2. Comparative analysis of nuclear events during conjugation in closely related species

The process of conjugation in *P. jenningsi* was first reported by Mitchell (1962, 1963). Later Fokin et al. (2001) provided more details, but all three studies only gave a textual description. Compared to previous reports, our findings are consistent with Mitchell's description, but in contrast with that of Fokin in two respects: (1) the two MICs in the prophase of meiosis I have a typical parachute form instead of a crescent shape; and (2) a variable number of nuclei undergo the third prezygotic division rather than only one.

In eukaryotes, chromatins take on different forms during their pairing movements at the meiotic prophase stage (Loidl, 2016), such as the classical bouquet arrangement (Zickler, 2006), or the horsetail shape of *Schizosaccharomyces pombe* (Yamamoto and Hiraoka, 2001). In ciliates, the prevalent chromosomal form during the prophase of meiosis is the "crescent" or "parachute" shape (Gong et al., 2022; Hanke-Bücker and Hauser, 1996; Tian et al., 2022). Most *Paramecium* species exhibit the "crescent" form (Fig. 5), including the *P. aurelia* complex (Fokin et al., 2001; Sugai, 1976). Although previous reports described the presence of the "crescent" form in *P. jenningsi* (Fokin et al., 2001), in our observations we only identified the typical "parachute" shape (Fig. 2). Recent studies have suggested that *P. jenningsi* is a complex of three isolated reproductive groups (Przyboś and Tarcz, 2016), which have been denoted *P. primjenningsi*, *P. bijenningsi*, and *P. trijenningsi*. Based on phylogenetic analyses, *P. jenningsi* strain GZ was assigned to *P. trijenningsi* (Figs. S1 and S2). These findings suggest that the difference between the present and previous observations may be attributed to the use of different cryptic species of *P. jenningsi* or the difference in degree of aging of the strains used.

Paramecium jenningsi is very closely related to sibling species of the *P. aurelia* complex. Members of the *P. aurelia* complex, however, share a similar conjugation process (Fokin et al., 2001), which is distinct from that of *P. jenningsi* (Fig. 5). The main differences are related to: (1) the morphology of the nucleus at the prophase of the first meiotic division (parachute vs. crescent); (2) the number of MIC that perform the third prezygotic division (variable vs. one); and (3) the number of nuclear products after the first postzygotic division that undergo degradation (one vs. zero).

4.3. Diversity of conjugation processes in the class oligohymenophorea

In order to gain a deeper understanding of the diversity and evolution of the conjugation process, we conducted a comparative analysis in 23 representative species of the class Oligohymenophorea, including symbiotic (*Mantoscyphidia branchi* and *Urceolaria synaptae*), facultative parasitic (*Uronema marinum*), sessile (*Vorticella microstoma* and *Carchesium polypinum*), and free-living species. The 23 representative species used in the comparison branch into two different clades of the SSU rDNA gene tree (Fig. 5). One clade includes the facultative parasitic *U. marinum* and 17 other free-living species, while the other clade includes five

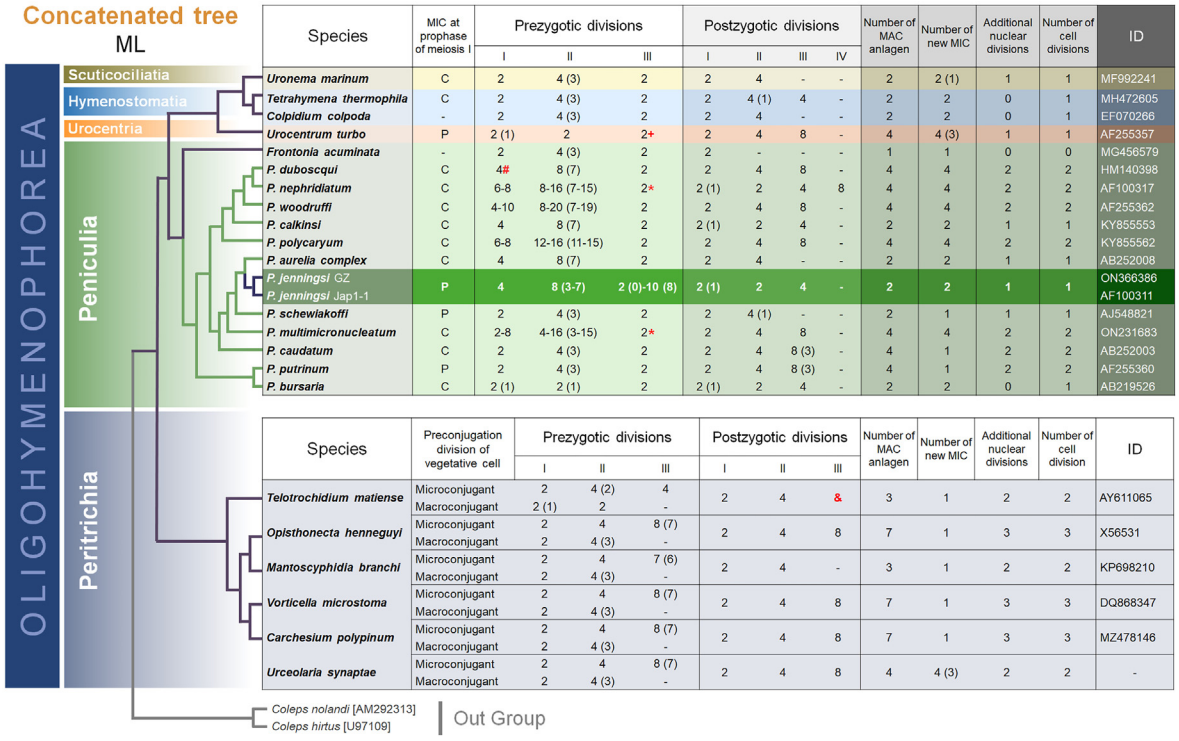

Species	MIC at prophase of meiosis I	Prezygotic divisions I	II	III	Postzygotic divisions I	II	III	IV	Number of MAC anlagen	Number of new MIC	Additional nuclear divisions	Number of cell divisions	ID
Uronema marinum	C	2	4 (3)	2	2	4	-	-	2	2 (1)	1	1	MF992241
Tetrahymena thermophila	C	2	4 (3)	2	2	4 (1)	4	-	2	2	0	1	MH472605
Colpidium colpoda	-	2	4 (3)	2	2	4	-	-	2	2	0	1	EF070266
Urocentrum turbo	P	2 (1)	2	2+	2	4	8	-	4	4 (3)	1	1	AF255357
Frontonia acuminata	-	2	4 (3)	2	2	-	-	-	1	1	0	0	MG456579
P. duboscqui	C	4#	8 (7)	2	2	4	8	-	4	4	2	2	HM140398
P. nephridiatum	C	6-8	8-16 (7-15)	2*	2 (1)	2	4	8	4	4	2	2	AF100317
P. woodruffi	C	4-10	8-20 (7-19)	2	2	4	8	-	4	4	2	2	AF255362
P. calkinsi	C	4	8 (7)	2	2 (1)	2	4	-	2	2	1	1	KY855553
P. polycaryum	C	6-8	12-16 (11-15)	2	2	4	8	-	4	4	2	2	KY855562
P. aurelia complex	C	4	8 (7)	2	2	4	-	-	2	2	1	1	AB252008
P. jenningsi GZ	P	4	8 (3-7)	2 (0)-10 (8)	2 (1)	2	4	-	2	2	1	1	ON366386
P. jenningsi Jap1-1													AF100311
P. schewiakoffi	P	2	4 (3)	2	2	4 (1)	-	-	2	1	1	1	AJ548821
P. multimicronucleatum	C	2-8	4-16 (3-15)	2*	2	4	8	-	4	4	2	2	ON231683
P. caudatum	C	2	4 (3)	2	2	4	8 (3)	-	4	1	2	2	AB252003
P. putrinum	P	2	4 (3)	2	2	4	8 (3)	-	4	1	2	2	AF255360
P. bursaria	C	2 (1)	2 (1)	2	2 (1)	2	4	-	2	2	0	1	AB219526

Species	Preconjugation division of vegetative cell	Prezygotic divisions I	II	III	Postzygotic divisions I	II	III	Number of MAC anlagen	Number of new MIC	Additional nuclear divisions	Number of cell division	ID
Telotrochidium matiense	Microconjugant	2	4 (2)	4	2	4	&	3	1	2	2	AY611065
	Macroconjugant	2 (1)	2	-								
Opisthonecta henneguyi	Microconjugant	2	4	8 (7)	2	4	8	7	1	3	3	X56531
	Macroconjugant	2	4 (3)	-								
Mantoscyphidia branchi	Microconjugant	2	4	7 (6)	2	4	-	3	1	2	2	KP698210
	Macroconjugant	2	4 (3)	-								
Vorticella microstoma	Microconjugant	2	4	8 (7)	2	4	8	7	1	3	3	DQ868347
	Macroconjugant	2	4 (3)	-								
Carchesium polypinum	Microconjugant	2	4	8 (7)	2	4	8	7	1	3	3	MZ478146
	Macroconjugant	2	4 (3)	-								
Urceolaria synaptae	Microconjugant	2	4	8 (7)	2	4	8	4	4 (3)	2	2	-
	Macroconjugant	2	4 (3)	-								

Fig. 5. Patterns of nuclear events during conjugation in representatives of the class Oligohymenophorea. The topology was drawn based on the phylogenomic analyses (at the subclass level according to Wang et al., 2021) and SSU rDNA (at the genus level). C: the micronucleus experiences the "crescent" stage during meiosis. P: the micronucleus experiences the "parachute" stage during meiosis. Numbers in brackets indicate the number of pyknotic nuclei. +: Refers to the incomplete third maturation division in *Urocentrum turbo*; #: after the first prezygotic division in *Paramecium duboscqui*, about 60% of cells contain four nuclear products according to Watanabe et al. (1996). *: refers to various meiotic products that undergo the third prezygotic division; &: the third postzygotic division may occasionally occur. The processes of conjugation are reviewed from the corresponding references: *Uronema marinum* (Coppellotti, 1990), *Tetrahymena thermophila* (Orias et al., 2011), *Colpidium colpoda* (Hoyer, 1899; Raikov, 1972), *Urocentrum turbo* (Serrano et al., 1987), *Frontonia acuminata* (Raikov, 1972), *P. duboscqui* (Watanabe et al., 1996), *P. nephridiatum* (Jankowski, 1961), *P. woodruffi* (Fokin et al., 2001), *P. calkinsi* (Nakata, 1956), *P. polycaryum* (Diller, 1958), *P. aurelia* complex (Diller, 1936; Fokin et al., 2001; Sonneborn, 1938), *P. jenningsi* GZ (the present work) (the SSU rRNA gene sequence of *P. jenningsi* Jap1-1 was used only for phylogenetic tree construction), *P. schewiakoffi* (Fokin et al., 2001), *P. multimicronucleatum* (Zhang et al., 2022), *P. caudatum* (Yang et al., 2007), *P. putrinum* (Jankowski, 1972), *P. bursaria* (Wichterman, 1948), *Telotrochidium matiense* (Martín-Cereceda et al., 2007), *Opisthonecta henneguyi* (Rosenberg, 1940), *Mantoscyphidia branchi* (Peters et al., 2010), *Vorticella microstoma* (Peters, 2002), *Carchesium polypinum* (Raikov, 1972), *Urceolaria synaptae* (Colwin, 1944).

Peritrichia species. No SSU rDNA sequence information is available for *U. synaptae*.

We found that all the species of the first clade undergo three prezygotic divisions in the same sequence (meiosis I, meiosis II, and mitosis). In most of them, only one meiosis product undergoes the subsequent mitosis, the exceptions being *Urocentrum turbo* (Serrano et al., 1987), *P. nephridiatum* (Jankowski, 1961), *P. multimicronucleatum* (Zhang et al., 2022) and *P. jenningsi* strain GZ. In the three *Paramecium* species, more than one meiotic product typically undergoes the third prezygotic division (Fig. 5); in *U. turbo*, the last (third) division is incomplete, since pronuclei are exchanged between cells during the metaphase of mitosis (Serrano et al., 1987). In all of these species, both the stationary and migratory pronuclei originate from the same product of the last mitotic division, resulting in their genetic identity. In *Euplotes*, the pronuclei are genetically different, as the sequence of prezygotic divisions starts with mitosis, followed by meiosis I and II. Consequently, the pronuclei derive from two of the eight meiotic products (Jiang et al., 2019). It is noteworthy that in roughly 75% of the above oligohymenophoreans that have been studied, the crescent phase dominates the MICs during the prophase of meiosis I. The remaining 25%, including *P. jenningsi* strain GZ, *P. schewiakoffi*, *P. putrinum*, and *U. turbo*, are dominated by the "parachute" phase (Fokin et al., 2001; Jankowski, 1972; Serrano et al., 1987).

In Peritrichia species, such as *Telotrochidium matiense* (Martín-Cereceda et al., 2007), *Opisthonecta henneguyi* (Rosenberg, 1940), *M. branchi* (Peters et al., 2010), *V. microstoma* (Peters, 2002), *C. polypinum* (Raikov, 1972) and *U. synaptae* (Colwin, 1944), the prezygotic divisions differ from those of most other free-living oligohymenophoreans because the two mating cells are of different sizes, with a stationary macroconjugant and a motile microconjugant. The MIC undergoes three divisions in the microconjugant but only two in the macroconjugant. One gametic pronucleus is retained in each cell (in contrast to other oligohymenophoreans, which retain two nuclei per cell), and a synkaryon is formed through the fusion of the genetically distinct pronuclei. Overall, three prezygotic divisions represent a general rule, although the of selection process for generating gametic pronuclei is distinct in different species.

The postzygotic divisions are more variable (Fig. 5). Among the 23 oligohymenophoreans investigated here, the synkaryon undergoes three postzygotic divisions in over 70% (including *P. jenningsi*), two postzygotic divisions in about 20%, and four two postzygotic divisions only in *P. nephridiatum*. In addition to postzygotic divisions, extra nuclear divisions and sometimes cell divisions occur in exconjugant cells before restoring the vegetative phase, depending on the initial ratio of new MIC to MAC anlagen and the number of each. In nearly 50% of oligohymenophoreans, of which more than 90% are free-living species, redundant nuclear products are degraded, but in different stages, i.e., before the first postzygotic division in *P. jenningsi* strain GZ, *P. bursaria*, *P. calkinsi*, and *P. nephridiatum*; after the first postzygotic division in *T. thermophila* and *P. schewiakoffi*; before the third postzygotic division in *P. caudatum* and *P. putrinum*; and after the complete postzygotic divisions in *U. marinum*, *U. turbo*, and *U. synaptae*. In Peritrichia species, no nuclear degradation occurs during the postzygotic divisions. *Frontonia acuminata* is the only species known to take one postzygotic division to complete the whole

conjugation process without the need extra cell division and nuclear degradation (Raikov, 1972).

Funding

This work was supported by the National Natural Science Foundation of China (No. 32270539, 31961123002), the Natural Science Foundation of Shandong Province (ZR2020JQ13), the Fundamental Research Funds for the Central Universities (202141004), and the Researchers Supporting Project Number (RSP2023R10) King Saud University, Riyadh, Saudi Arabia.

Author contributions

Xue Zhang: conceptualization, data curation, formal analysis, investigation, methodology, writing original draft, review, and editing. Ruitao Gong: formal analysis, writing-review. Yaohan Jiang: conceptualization, formal analysis, writing-original draft, reviewing editing, and validation. Xiaoteng Lu: writing-review and editing. Chenyin Wu: Investigation. Lihan Wang: investigation. Hongwei Ma: investigation. Zhengxiang Zhang: investigation. Weibo Song: writing-review and editing. Khaled A. S. Al-Rasheid, funding acquisition. Adriana Vallesi: writing-review and editing. Feng Gao: writing-review and editing, funding acquisition, supervision and validation.

Declaration of competing interest

The authors declare that they have no known competing financial interests or personal relationships that could have appeared to influence the work reported in this paper. Weibo Song is an editorial board member for Water Biology and Security and was not involved in the editorial review or the decision to publish this article.

Acknowledgement

Our sincere thanks are given to our colleague, Mr. Yong Chi (OUC), for his kind help in species identification.

Appendix A. Supplementary data

Supplementary data to this article can be found online at https://doi.org/10.1016/j.watbs.2023.100201.

References

Akematsu, T., Sánchez-Fernández, R., Kosta, F., Holzer, E., Loidl, J., 2020. The transmembrane protein Semi1 positions gamete nuclei for reciprocal fertilization in *Tetrahymena*. iScience 23 (1), 100749.

Allen, S.L., Nerad, T.A., Rushford, C.L., 1983. Comparison of the esterases and acid phosphatases in *Paramecium multimicronucleatum*, syngens 1–5, *P. jenningsi, P. caudatum*, and the *P. aurelia* complex. J. Protozool. 30 (1), 148–154.

Aufderheide, K.J., Daggett, P.M., Nerad, T.A., 1983. *Paramecium sonneborni* n. sp., a new member of the *Paramecium aurelia* species-complex. J. Protozool. 30 (1), 128–131.

Aury, J.M., Jaillon, O., Duret, L., Noel, B., Jubin, C., Porcel, B.M., Ségurens, B., Daubin, V., Anthouard, V., Aiach, N., et al., 2006. Global trends of whole-genome duplications revealed by the ciliate *Paramecium tetraurelia*. Nature 444 (7116), 171–178.

Bai, S.N., 2015. The concept of the sexual reproduction cycle and its evolutionary significance. Front. Plant Sci. 6, 11.

Barth, D., Przyboś, E., Fokin, S.I., Schlegel, M., Berendonk, T.U., 2008. Cytochrome b sequence data suggest rapid speciation within the *Paramecium aurelia* species complex. Mol. Phylogenet. Evol. 49 (2), 669–673.

Cavalier-Smith, T., 2002. Origins of the machinery of recombination and sex. Heredity 88 (2), 125–141.

Cervantes, M.D., Hamilton, E.P., Xiong, J., Lawson, M.J., Yuan, D., Hadjithomas, M., Miao, W., Orias, E., 2013. Selecting one of several mating types through gene segment joining and deletion in *Tetrahymena thermophila*. PLoS Biol. 11 (3), e1001518.

Chau, M.F., Ng, S.F., 1988. The somatic function of the micronucleus in asexual reproduction of *Paramecium*: thermosensitivity of amicronucleates. Biol. Cell. 62 (3), 219–227.

Chen, X., Jiang, Y.H., Gao, F., Zheng, W.B., Krock, T.J., Stover, N.A., Lu, C., Katz, L.A., Song, W.B., 2019. Genome analyses of the new model protist *Euplotes vannus* focusing on genome rearrangement and resistance to environmental stressors. Mol Ecol Resour 19 (5), 1292–1308.

Chi, Y., Wang, Z., Ye, T.T., Wang, Y., Zhao, J.L., Song, W.B., Bourland, W.A., Chen, X.R., 2022. A new contribution to the taxonomy and phylogeny of the ciliate genus *Spirostomum* (Alveolata, Ciliophora, Heterotrichea), with comprehensive descriptions of two species from wetlands in China. Water Biol. Syst. 1 (2), 100031.

Chowdhury, D., Keogh, M.C., Ishii, H., Peterson, C.L., Buratowski, S., Lieberman, J., 2005. γ-H2AX dephosphorylation by protein phosphatase 2A facilitates DNA double-strand break repair. Mol. Cell 20 (5), 801–809.

Colwin, L.H., 1944. Binary fission and conjugation in *Urceolaria synaptae* (?) type II (Protozoa, Ciliata) with special reference to the nuclear phenomena. J. Morphol. 75 (2), 203–249.

Coppellotti, O., 1990. Description of *Uronema marinum* (Ciliophora, Scuticociliatida) from the Antarctica and observations on the nuclear events in conjugation. Polar Biol. 10 (5), 365–371.

Diller, W.F., 1936. Nuclear reorganization processes in *Paramecium aurelia*, with descriptions of autogamy and 'hemixis'. J. Morphol. 59 (1), 11–67.

Diller, W.F., 1958. Studies on conjugation in *Paramecium polycaryum*. J. Protozool. 5 (4), 282–292.

Diller, W.F., Earl, P.R., 1958. *Paramecium jenningsi*, n. sp. J. Protozool. 5 (2), 155–158.

Dryl, S., 1959. Antigenic transformation in *Paramecium aurelia* after homologous antiserum treatment during autogamy and conjugation. J. Protozool. 6 (Suppl. l), 25.

Duan, L.L., Cheng, T., Wei, F., Qiao, Y., Wang, C.C., Warren, A., Niu, J.H., Wang, Y.Y., 2021. New contribution to epigenetic studies: isolation of micronuclei with high purity and DNA integrity in the model ciliated protist, *Tetrahymena thermophila*. Eur. J. Protistol. 80, 125804.

Fokin, S.I., Przybos, E., Chivilev, S.M., 2001. Nuclear reorganization variety in *Paramecium* (Ciliophora: peniculida) and its possible evolution. Acta Protozool. 40 (4), 249–262.

Fokin, S.I., Przyboś, E., Chivilev, S.M., Beier, C.L., Horn, M., Skotarczak, B., Wodecka, B., Fujishima, M., 2004. Morphological and molecular investigations of *Paramecium schewiakoffi* sp. nov. (Ciliophora, Oligohymenophorea) and current status of distribution and taxonomy of *Paramecium* spp. Eur. J. Protistol. 40 (3), 225–243.

Fu, J.Y., Chi, Y., Lu, X.T., Gao, F., Al-Farraj, S.A., Petroni, G., Jiang, J.M., 2022. Doublets of the unicellular organism *Euplotes vannus* (Alveolata, Ciliophora, Euplotida): the morphogenetic patterns of the ciliary and nuclear apparatuses associated with cell division. Mar. Life Sci. Technol. 4 (4), 527–535.

Fujishima, M., 1983. Microspectrophotometric and autoradiographic study of the timing and duration of pre-meiotic DNA synthesis in *Paramecium caudatum*. J. Cell Sci. 60 (1), 51–65.

Fujishima, M., Hiwatashi, K., 1977. An early step in initiation of fertilization in *Paramecium*: early micronuclear migration. J. Exp. Zool. 201 (1), 127–133.

Fujishima, M., Watanabe, T., 1981. Transplantation of germ nuclei in *Paramecium caudatum*: III. Role of germinal micronucleus in vegetative growth. Exp. Cell Res. 132 (1), 47–56.

Gong, R.T., Chi, Y., Shao, C., Yuan, Q.X., Li, Y.Q., Warren, A., Wang, Y.R., 2022. Conjugation in the eukaryotic single-celled organism *Euplotes aediculatus* (Protozoa, Ciliophora): a focus on nuclear divisions, morphogenesis and pheromones. J. King Saud Univ. Sci. 34, 102091.

Gong, R.T., Jiang, Y.H., Vallesi, A., Gao, Y.Y., Gao, F., 2020. Conjugation in *Euplotes raikovi* (Protista, Ciliophora): new insights into nuclear events and macronuclear development from micronucleate and amicronucleate cells. Microorganisms 8 (2), 162.

Goodenough, U., Heitman, J., 2014. Origins of eukaryotic sexual reproduction. Cold Spring Harbor Perspect. Biol. 6 (3), a016154.

Grandchamp, S., Beisson, J., 1981. Positional control of nuclear differentiation in *Paramecium*. Dev. Biol. 81 (2), 336–341.

Hall, T., 1999. BioEdit: a user-friendly biological sequence alignment editor and analysis program for Windows 95/98/NT. Nucleic Acids Symp. Ser. 41, 95–98.

Hanke-Bücker, G., Hauser, M., 1996. Nuclear phenomena during conjugation of the suctorian *Heliophrya erhardi*: I. EM-observations of micronuclear meiosis. Eur. J. Protistol. 32 (4), 459–480.

Hiwatashi, K., 1968. Determination and inheritance of mating type in *Paramecium caudatum*. Genetics 58 (3), 373–386.

Hiwatashi, K., Mikami, K., 1989. Fertilization in *Paramecium*: processes of the nuclear reorganization. Int. Rev. Cytol. 114, 1–19.

Hoyer, H., 1899. Ueber das Verhalten der Kerne bei der Conjugation des Infusors *Colpidium colpoda* St. Arch. Mikrosk. Anat. 54 (1), 95–134 (in German).

Iwamoto, M., Koujin, T., Osakada, H., Mori, C., Kojidani, T., Matsuda, A., Asakawa, H., Hiraoka, Y., Haraguchi, T., 2015. Biased assembly of the nuclear pore complex is required for somatic and germline nuclear differentiation in *Tetrahymena*. J. Cell Sci. 128 (9), 1812–1823.

Jahn, C.L., Klobutcher, L.A., 2002. Genome remodeling in ciliated protozoa. Annu. Rev. Microbiol. 56 (1), 489–520.

Jankowski, A.W., 1961. The process of conjugation in the rare salt water *Paramecium*. P. woodruffi. Dokl. Akad. Nauk SSSR 137, 989–992.

Jankowski, A.W., 1972. Cytogenetics of *Paramecium putrinum* C. et L., 1858. Acta Protozool. 10 (17), 285–394.

Jiang, Y.H., Zhang, T.T., Vallesi, A., Yang, X.Y., Gao, F., 2019. Time-course analysis of nuclear events during conjugation in the marine ciliate *Euplotes vannus* and comparison with other ciliates (Protozoa, Ciliophora). Cell Cycle 18 (3), 288–298.

Knoll, A.H., 2014. Paleobiological perspectives on early eukaryotic evolution. Cold Spring Harbor Perspect. Biol. 6 (1), a016121.

Kovalchuk, I., 2021. From micronucleus to macronucleus: programmed DNA rearrangement in ciliates is regulated by non-coding RNA molecules. In:

Kovalchuk, I., Kovalchuk, O. (Eds.), Genome Stability, second ed. Academic Press, New York, USA, pp. 109–123.
Kumar, S., Stecher, G., Tamura, K., 2016. MEGA7: molecular evolutionary genetics analysis version 7.0 for bigger datasets. Mol. Biol. Evol. 33 (7), 1870–1874.
Li, T., Liu, M.J., Warren, A., Al-Farraj, S.A., Yi, Z.Z., Sheng, Y.L., 2022. Morphology and SSU rRNA gene-based phylogeny of three peniculid ciliates (Ciliophora, Oligohymenophorea) from China, including a new *Frontonia* species. Eur. J. Protistol. 85, 125910.
Lipps, H.J., Postberg, J., Jackson, D.A., Mochizuki, K., 2010. RNA-directed epigenetic regulation of DNA rearrangements. Essays Biochem. 48, 89–100.
Loidl, J., 2016. Conservation and variability of meiosis across the eukaryotes. Annu. Rev. Genet. 50, 293–316.
Luporini, P., Alimenti, C., Ortenzi, C., Vallesi, A., 2005. Ciliate mating types and their specific protein pheromones. Acta Protozool. 44, 89–101.
Luporini, P., Pedrini, B., Alimenti, C., Vallesi, A., 2016. Revisiting fifty years of research on pheromone signaling in ciliates. Eur. J. Protistol. 55, 26–38.
Lynn, D.H., 2008. The Ciliated Protozoa: Characterization, Classification, and Guide to the Literature, third ed. Springer, Dordrecht, The Netherlands.
Ma, M.Z., Li, Y.Q., Maurer-Alcala, X., Wang, Y.R., Yan, Y., 2022a. Deciphering phylogenetic relationships in class Karyorelictea (Protista, Ciliophora) based on updated multi-gene information with establishment of a new order Wilbertomorphida n. ord. Mol. Phylogenet. Evol. 169, 107406.
Ma, M.Z., Xu, Y., Lu, B.R., Li, Y.Q., Song, W.B., Petroni, G., Al-Farrah, S.A., Yan, Y., 2022b. Molecular Phylogeny and taxonomy of four *Remanella* species (Protozoa, Ciliophora): a flagship genus of karyorelictean ciliates, with descriptions of three new species. Zool. Res. 43, 827–842.
Martín-Cereceda, M., Guinea, A., Bonaccorso, E., Dyal, P., Novarino, G., Foissner, W., 2007. Classification of the peritrich ciliate *Opisthonecta matiensis* (Martín-Cereceda et al. 1999) as *Telotrochidium matiense* nov. comb., based on new observations and SSU rDNA phylogeny. Eur. J. Protistol. 43 (4), 265–279.
Mikami, K., 1980. Differentiation of somatic and germinal nuclei correlated with intracellular localization in *Paramecium caudatum* exconjugants. Dev. Biol. 80 (1), 46–55.
Miller, M.A., Pfeiffer, W., Schwartz, T., 2010. Creating the CIPRES Science Gateway for Inference of Large Phylogenetic Trees. Gateway Computing Environments Workshop (GCE). 1–8 (New Orleans, LA).
Mitchell, J., 1962. Nuclear reorganization in *Paramecium jenningsi*. J. Protozool. 9, 26.
Mitchell, J., 1963. Nuclear activity in *Paramecium jenningsi* with reference to other members of the aurelia group. J. Protozool. 10 (Suppl. l), 11.
Nakata, A., 1956. Micronuclear behavior during the conjugation of *Haramecium calkinsi*. Doubutsugaku Zasshi 65 (8), 306–310 (in Japanese with English abstract).
Nanney, D.L., 1953a. Mating type determination in *Paramecium aurelia*, a model of nucleo-cytoplasmic interaction. Proc. Natl. Acad. Sci. USA 39 (2), 113.
Nanney, D.L., 1953b. Nucleo-cytoplasmic interaction during conjugation in *Tetrahymena*. Biol. Bull. 105 (1), 133–148.
Ng, S.F., Fujishima, M., 1989. Control of development of the oral apparatus of *Paramecium* during sexual reproduction: an embryological perspective. Dev. Biol. 134 (2), 317–326.
Orias, E., 1986. Ciliate conjugation. In: Gall, J.G. (Ed.), The Molecular Biology of Ciliated Protozoa. Academic Press, New York, USA, pp. 45–85.
Orias, E., Cervantes, M.D., Hamilton, E.P., 2011. *Tetrahymena thermophila*, a unicellular eukaryote with separate germline and somatic genomes. Res. Microbiol. 162 (6), 578–586.
Orias, E., Singh, D.P., Meyer, E., 2017. Genetics and epigenetics of mating type determination in *Paramecium* and *Tetrahymena*. Annu. Rev. Microbiol. 71, 133–156.
Peters, H., 2002. Reproductive Processes of Scyphidiid Peritrichs Associated with Limpet and Haliotid Hosts along the Coast of South Africa. University of the Free State.
Peters, H., Van As, L.L., Basson, L., 2010. Binary fission, telotroch formation and conjugation in *Mantoscyphidia* Jankowski, 1980 (Ciliophora: Peritrichia). Acta Protozool. 49 (1), 61–74.
Phadke, S.S., Zufall, R.A., 2009. Rapid diversification of mating systems in ciliates. Biol J Linn Soc Lond 98 (1), 187–197.
Potekhin, A., Mayén-Estrada, R., 2020. *Paramecium* diversity and a new member of the *Paramecium aurelia* species complex described from Mexico. Diversity 12 (5), 197.
Prescott, D.M., 1994. The DNA of ciliated protozoa. Microbiol. Rev. 58 (2), 233–267.
Przyboś, E., Tarcz, S., 2016. *Paramecium jenningsi* complex: existence of three cryptic species confirmed by multi-locus analysis and strain crosses. Syst. Biodivers. 14 (2), 140–154.
Przyboś, E., Tarcz, S., Rautian, M., Sawka, N., 2015. Delimiting species boundaries within a paraphyletic species complex: insights from morphological, genetic, and molecular data on *Paramecium sonneborni (Paramecium aurelia* species complex, Ciliophora, Protozoa). Protist 166 (4), 438–456.
Raikov, I.B., 1972. Nuclear Phenomena during Conjugation and Autogamy in Ciliates. Pergamon Press, New York, USA.
Raikov, I.B., 1982. The Protozoan Nucleus: Morphology and Evolution. Springer-Verlag, Vienna, Austria.
Rosenberg, L.E., 1940. Conjugation in "*Opisthonecta henneguyi*" a free swimming vorticellid. Proc. Am. Phil. Soc. 437–448.
Sawka-Gądek, N., Potekhin, A., Singh, D.P., Grevtseva, I., Arnaiz, O., Penel, S., Sperling, L., Tarcz, S., Duret, L., Nekrasova, I., et al., 2021. Evolutionary plasticity of mating-type determination mechanisms in *Paramecium aurelia* sibling species. Genome Biol. Evol. 13 (2), evaa258.
Sela, I., Ashkenazy, H., Katoh, K., Pupko, T., 2015. GUIDANCE2: accurate detection of unreliable alignment regions accounting for the uncertainty of multiple parameters. Nucleic Acids Res. 43 (W1). W7–W14.
Serrano, S., Martin-Gonzalez, A., Fernández-Galiano, D., 1987. Nuclear phenomena and oral reorganization during the conjugation of *Urocentrum turbo* O. F. M (Ciliata). Arch. Protistendk. 133 (3–4), 257–268.
Sheng, Y.L., Duan, L.L., Cheng, T., Qiao, Y., Stover, N.A., Gao, S., 2020. The completed macronuclear genome of a model ciliate *Tetrahymena thermophila* and its application in genome scrambling and copy number analyses. Sci. China Life Sci. 63 (10), 1534–1542.
Sheng, Y.L., Pan, B., Wei, F., Wang, Y.Y., Gao, S., 2021. Case study of the response of N6-methyladenine DNA modification to environmental stressors in the unicellular eukaryote *Tetrahymena thermophila*. mSphere 6 (3), e01208–01220.
Shi, L., Oberdoerffer, P., 2012. Chromatin dynamics in DNA double-strand break repair. Biochim. Biophys. Acta Gene Regul. Mech. 1819 (7), 811–819.
Song, W.Y., Luo, X.T., Chi, Y., Al-Farraj, S.A., Shao, C., 2022. Ontogenesis and systematic position of a new hypotrichous ciliate, *Chaetospira sinica* sp. nov., with an improved diagnosis of the poorly defined family Chaetospiridae Jankowski, 1985 (Protozoa, Ciliophora, Hypotrichia). Mar. Life Sci. Technol. 4 (4), 513–526.
Sonneborn, T.M., 1938. Mating types in *Paramecium aurelia*: diverse conditions for mating in different stocks; occurrence, number and interrelations of the types. Proc. Am. Phil. Soc. 411–434.
Sonneborn, T.M., 1951. Some current problems of genetics in the light of investigations on *Chlamydomonas* and *Paramecium*. Cold Spring Harbor Symp. Quant. Biol. 16, 483–503.
Sonneborn, T.M., 1975. The *Paramecium aurelia* complex of fourteen sibling species. Trans. Am. Microsc. Soc. 155–178.
Sugai, T., 1976. Chromosomal association and arrangement at meiotic prophase of the micronucleus in *Paramecium*. Jpn. J. Genet. 51 (6), 385–392.
Tian, M., Cai, X., Liu, Y.J., Liucong, M.M., Howard-Till, R., 2022. A practical reference for studying meiosis in the model ciliate *Tetrahymena thermophila*. Mar. Life Sci. Technol. 4 (4), 595–608.
Wang, C.D., Gao, Y.Y., Lu, B.R., Chi, Y., Zhang, T.T., El-Serehy, H.A., Al-Farraj, S.A., Li, L.F., Song, W.B., Gao, F., 2021. Large-scale phylogenomic analysis provides new insights into the phylogeny of the class Oligohymenophorea (Protista, Ciliophora) with establishment of a new subclass Urocentria nov. subcl. Mol. Phylogenet. Evol. 159, 107112.
Wang, Z., Chi, Y., Li, T., Song, W.Y., Wang, Y.F., Wu, T., Zhang, G.A.T., Liu, Y.J., Ma, H.G., Song, W.B., 2022. Biodiversity of freshwater ciliates (protista, Ciliophora) in the lake weishan wetland, China: the state of the art. Mar. Life Sci. Technol. 4 (4), 429–451.
Watanabe, T., Shi, X.B., Liu, G.J., Jin, M.L., 1996. Cytological studies of conjugation and nuclear processes in *Paramecium duboscqui* Chatton & Brachon 1933. Eur. J. Protistol. 32, 175–182.
Wichterman, R., 1948. The time schedule of mating and nuclear events in the conjugation of *Paramecium bursaria*. Turtox News 26, 2–10.
Yamamoto, A., Hiraoka, Y., 2001. How do meiotic chromosomes meet their homologous partners?: lessons from fission yeast. Bioessays 23 (6), 526–533.
Yamauchi, K., Tada, H., Usuki, I., 1995. Structure and evolution of *Paramecium* hemoglobin genes. Biochim. Biophys. Acta Gene Regul. Mech. 1264 (1), 53–62.
Yanagi, A., 1987. Positional control of the fates of nuclei produced after meiosis in *Paramecium caudatum*: analysis by nuclear transplantation. Dev. Biol. 122 (2), 535–539.
Yang, X.Y., Gao, X., Shi, X.L., 2007. Detection of haploid nuclear death in living *Paramecium caudatum*. Jpn. J. Protozool. 40 (2), 123–130.
Yang, X.Y., Takahashi, M., 1999. Disturbance of the determination of germinal and somatic nuclei by heat shock in *Paramecium caudatum*. J. Eukaryot. Microbiol. 46 (1), 49–55.
Yang, X.Y., Takahashi, M., 2000. Nutrient supply induces germinal nuclear selection in exconjugants of *Paramecium caudatum*. Proc. Jpn. Acad., Ser. B 76 (7), 87–91.
Yang, X.Y., Takahashi, M., 2002. Nuclei may anchor at specific locations during nuclear determination in *Paramecium caudatum*. Eur. J. Protistol. 38 (2), 147–153.
Zhang, D., Gao, F., Jakovlić, I., Zou, H., Zhang, J., Li, W.X., Wang, G.T., 2020. PhyloSuite: an integrated and scalable desktop platform for streamlined molecular sequence data management and evolutionary phylogenetics studies. Mol. Ecol. Resour. 20 (1), 348–355.
Zhang, X., Lu, X.T., Chi, Y., Jiang, Y.H., Wang, C.D., Al-Farraj, S.A., Vallesi, A., Gao, F., 2022. Timing and characteristics of nuclear events during conjugation and genomic exclusion in *Paramecium multimicronucleatum*. Mar. Life Sci. Technol. 4 (3), 317–328.
Zhao, L., Gao, F., Gao, S., Liang, Y.J., Long, H.A., Lv, Z.Y., Su, Y., Ye, N.H., Zhang, L.S., Zhao, C.T., et al., 2021. Biodiversity-based development and evolution: the emerging research systems in model and non-model organisms. Sci. China Life Sci. 64 (8), 1236–1280.
Zheng, W.B., Chen, J., Doak, T.G., Song, W.B., Yan, Y., 2020. ADFinder: accurate detection of programmed DNA elimination using NGS high-throughput sequencing data. Bioinformatics 36 (12), 3632–3636.
Zickler, D., 2006. From early homologue recognition to synaptonemal complex formation. Chromosoma 115 (3), 158–174.